PNAS

www.pnas.org

Supplementary Information for

Multifunctionalized hydrogels foster hNSC maturation in 3D cultures and neural regeneration in spinal cord injuries

Amanda Marchini[a,b,1], Andrea Raspa[a,1], Raffaele Pugliese[a], Marina Abd El Malek[b], Valentina Pastori[c], Marzia Lecchi[c], Angelo L. Vescovi[a], Fabrizio Gelain[a,b,2]

[a]Unità Ingegneria Tissutale, Fondazione Istituto di Ricovero e Cura a Carattere Scientifico Casa Sollievo della Sofferenza, Unità Ingegneria Tissutale, 71013 Foggia, Italy

[b]Center for Nanomedicine and Tissue Engineering, ASST Ospedale Metropolitano Niguarda, 20162 Milan, Italy

[c]Department of Biotechnology and Biosciences, University of Milano-Bicocca, 20126 Milan, Italy

[1]A.M and A.R. contributed equally to this work

[2]To whom correspondence should be addressed. Email: f.gelain@css-mendel.it

This PDF file includes:

Supplementary Materials and Methods
Supplementary Figures S1-S7
Supplementary Table S1-S14
References for SI citations

SUPPLEMENTARY MATERIALS AND METHODS

hNSCs cultures. Cells were cultured in untreated flasks (Thermo Scientific) at density of 10^4 cells/cm^2 using serum-free medium in the presence of basic fibroblast growth factor (bFGF, PeproTech) and EGF (PeproTech) at final concentrations of 10 ng/ml and 20 ng/ml, respectively. Cell cultures were maintained in a humidified incubator at 37°C, 5% O_2 and 5% CO_2 to allow neurosphere generation (1, 2). Neurospheres were mechanically dissociated every 10 days in the same growth medium.

Samples preparation: hNSC-HYDROSAP and HYDROSAP. hNSC-HYDROSAP is a 3D culture system composed by a mixing solution containing 0.81 mM pureHYDROSAP (previously dissolved 1% w/v in distilled water, GIBCO), 280 mM sucrose solution, 2.5 mM NaOH and hNSCs (4.5 x 10^4 cells/µl). A droplet (40 µl) was placed onto glass coverslip in 24-well, serum-free medium supplemented with bFGF (20 ng/ml, Peprotech) was added to start SAP gelation and to obtain free-floating hNSC-HYDROSAP. At 2 DIV, medium was shifted to a basal medium supplemented with LIF (20 ng/ml, Chemicon) and BDNF (20 ng/ml, Peprotech) (3). In these conditions, the samples were maintained in culture up to different time-points (1, 2, 4, 6, 8, 10 weeks). Additionally, hNSC-HYDROSAP(1D) and T0 samples were maintained in culture for 24 hours and for 1 hour respectively. HYDROSAP sample was developed with the same components of hNSC-HYDROSAP but without cells.

Synthesis and purification of pureHYDROSAP. Linear SAPs Ac-(LDLK)$_3$-CONH$_2$, Ac-KLPGWSGGGG-(LDLK)$_3$-CONH$_2$ and Ac-SSLSVNDGGG-(LDLK)$_3$-CONH$_2$ (4, 5) and branched SAP tris(LDLK)$_3$-CONH$_2$ (6) were synthesized by solid-phase Fmoc-based chemistry on Rink amide 4-methyl-benzhydrylamine resin (0.5 mmol g^{-1} substitution) using the Liberty-Discovery (CEM) microwave automated synthesizer, as previously described (6). For all peptides the side chains removal and cleavage were performed with TFA:TIS:H2O (95:2.5:2.5) cocktail. Cleaved peptides were precipitated using cold ethyl ether and then lyophilized (Labconco). The resulting raw peptides have been purified by a Waters binary HPLC apparatus (>95%) and the molecular weight was confirmed via single quadrupole mass detection (Waters LC-MS Alliance-3100). Purified peptides

powder was subsequently dissolved in 0.1 M HCl in order to remove the presence of possible TFA salts.

CrossCK lamina preparation. Cross-linked SAP lamina (crossCK) was prepared as previously described (7). The day prior to the cross-linking reaction, Ac-CGGLKLKLKLKLKLKGGC-CONH$_2$ (named CK) SAP was dissolved at a concentration of 5% (w/v) in distilled water, sonicated for 20 minutes and incubated at 4°C for 24h. Right before the cross-linking reaction, 20mM of sulfo-SMCC (Thermofischer scientific) was dissolved in 1mL of DPBS (Thermofisher scientific 1X, w/o MgCl2 and CaCl2) and H$_2$O (1:1 v/v; pH 7.4) and subsequently added to CK peptide solution. Then, the cross-linking solution and CK peptide were cast on a disposable insert and incubated overnight at RT. At the end of the reaction, the un reacted sulfo-SMCC in the supernatant was removed by aspiration with a vacuum pipette, and the resulting crossCK lamina was washed and suspended in 1.5 mL of DPBS for 1 h. Washes were repeated 5 times before use.

Rheological measurements. Rheological properties of assembled nanostructures were carried out using a controlled stress AR-2000ex Rheometer (TA instruments). The instrument was equipped with a cone-plate geometry (acrylic truncated diameter, 20 mm; angle, 1°; truncation gap, 34 μm) (6). All measurements were performed at 25°C by using a Peltier cell as a lower plate of the instrument to control the temperature during each test.

Two samples were tested: 1) pureHYDROSAP (1% w/v); 2) HYDROSAP (components are described in "Samples preparation: hNSC-HYDROSAP and HYDROSAP" section). Time-sweep experiments were performed at constant angular frequency (ω=1Hz) to monitor the sol-gel transition, evaluating the storage (G') and loss (G") moduli increments as a function of time. Afterwards, frequency sweep experiments were recorded at a fixed 1% strain and as a function angular frequency (0.1-100Hz). Stress/strain sweeps were performed (0.01%-1000%) to identify the limits of the linear viscoelastic region and the failure stress of the samples. Viscosity plots were obtained by a shear rate ramp (0.001-1000 s^{-1}). Each experiment was performed in triplicate.

Atomic force microscopy (AFM) analysis. AFM morphological analyses were captured in tapping mode by a Multimode Nanoscope V (Digital Instrument, Veeco), using a single-beam silicon cantilever probes (Veeco RFESP MPP-21100-10, cantilever f_0, resonance frequency 59-69 KHz, constant force 3 N m^{-1}) (6). Peptide was dissolved in distilled water at the concentration of 1% (w/v) one day before imaging. Right before the analysis, peptide solution was diluted to a final concentration of 0.001% (w/v) and deposited on a freshly cleaved mica surface. A 2 µl of peptide solution was kept on mica for 4 min at RT and subsequently, the surface was rinsed with distilled water, to remove loosely bound peptides, and dried under RT for 30 min in a covered petri-dish, to protect from contamination until it was imaged.

Fourier transform infrared spectroscopy (FTIR) analysis. FTIR analysis of assembled nanostructures was performed on peptides dissolved at a concentration of 1% (w/v) in distilled water, after 24 h incubation at 4°C. All spectra were collected in attenuated total reflection (ATR) using Perkin Elmer Spectrum 100 spectrometer (6, 7). A 2 µl aliquot of each peptide solution was deposited on the reflection diamond element of the ATR-FTIR device and left to evaporate. Twenty acquisitions were recorded for each spectrum, using the following condition: 4 cm^{-1} spectrum resolution, 25 kHz scan speed, 1000 scan co-addition and a triangular apodization. All collected spectra were reported after ATR correction, smoothing and automatic baseline correction using Origin8™ software. Each sample was done in triplicate.

Thioflavin T (ThT) spectroscopy assay. ThT analysis of assembled peptides was performed to assess the presence of cross-β fibril structures (6).
ThT stock solution (Sigma- Aldrich, T3516) was prepared by adding 8 mg of ThT to 10 ml phosphate buffer (10 mM phosphate, 150 mM NaCl, pH 7) and filtered through a 0.2 µm syringe filter. Right before the analysis, 1 mL of ThT stock solution was diluted into 50 mL of phosphate buffer (working solution). Peptides at 1% (w/v) were mixed with working solution (1:0.5 v/v) and stirred for 2 min. ThT binding was monitored by

exciting the sample at 440 nm (5nm bandpass) and recording the emission fluorescence spectrum from 460 to 600 nm.

Immunofluorescence analyses *in vitro*. hNSC-HYDROSAPs were fixed with 4% paraformaldehyde (PFA), embedded in OCT and cryosectioned at 100 µm. Morphological evaluation was performed by Hematoxylin-Eosin staining. For immunofluorescence analyses, slices were washed in PBS, permeabilized with 0.3% Triton X-100 for 10 minutes at 4°C and treated with 10% normal goat serum (NGS, GIBCO) for 1 h at room temperature. The following primary antibodies were used: mouse antiβIII-Tubulin (βIII-TUB) (1:500, Biolegend), rabbit anti-glial fibrillary acidic protein (GFAP) (1:500, DAKO), mouse anti-galactocerebroside (GalC) (1:200, Millipore), mouse anti-oligodendrocytes marker O4 (1:200, Millipore), rabbit anti-growth associated protein-43 (GAP43) (1:1000, Millipore), mouse anti-neurofilament-H (SMI31) (1:1000, Biolegend), mouse anti-microtubule associated protein 2 (MAP2) (1:300, Invitrogen), rabbit anti-g-aminobutyric acid (GABA) (1:500, Sigma), rabbit anti-vescicular glutamate transporter 1 (VGLUT1) (1:500, Invitrogen), rabbit anti-choline acetyltransferase (ChAT, Invitrogen) (1:500), mouse anti-myelin basic protein (MBP) (1:2000, Biolegend), rabbit anti-nestin (1:500, Millipore) and rabbit anti-Ki67 (1:750, Invitrogen). To reveal primary antibodies, the following secondary antibodies were used: goat anti-rabbit Cy3 (1:1000, Jackson), goat anti-mouse Cy3 (1:1000, Jackson), goat anti-rabbit Alexa 488 (1:1000, Invitrogen) and goat anti-mouse Alexa 488 (1:1000, Invitrogen). Cell nuclei were counterstained with DAPI (Molecular Probes). Tunel assay (*In situ cell death detection kit fluorescein*, Roche) was performed to detect and quantify apoptotic cells. The protocol was performed following the manufacturer's instructions. Briefly, slices were permeabilized as previously described and incubated with Tunel reaction mixture (10% v/v enzyme solution) for 1 hour at 37°C.

A minimum of three randomly chosen fields of three independent experiments, per each timepoint and marker, were acquired at 40x magnification via Zeiss Microscope with Apotome System. Quantitative analyses were performed by counting manually positive cells for each marker using NIH-ImageJ software. Instead, representative images at 60X magnification were acquired using Nikon A1 Confocal Microscope.

Preparation of CULTREX 3D. CULTREX-BME® (R&D Systems) was used as in vitro positive control. To create a CULTREX 3D scaffold, the day after neurosphere dissociation, 87.5% v/v of CULTREX was mixed with 12.5% v/v of solution containing hNSCs (4.5×10^4 cells/µL final concentration). 40 µL of this mixture was placed in 24-well in the presence of basal medium supplemented with bFGF and maintained in incubator at 37°C with 5% CO_2 and 20% O_2. At 2 DIV, medium was shifted to the medium supplemented with LIF and BDNF. Samples were cultured up to different time-points (1, 2, 4, 6, 8 weeks). In vitro characterization was performed as described for hNSC-HYDROSAP.

Electrophysiology. At the abovementioned time-points, functional analyses of hNSC-HYDROSAP and CULTREX 3D were performed at 33-34°C while perfusing the culture at the rate of 2 ml/min with the oxygenated artificial cerebrospinal fluid, containing (in mM): 119 NaCl, 2.5 KCl, 2.5 $CaCl_2$, 1.3 $MgCl_2$, 26 $NaHCO_3$, 1.25 NaH_2PO_4 and 11 glucose. Cells were observed by a direct microscope (Eclipse E600FN), equipped with differential interference contrast (DIC) water immersion objective (Nikon), an infrared digital CCD camera, and HC Image Live acquisition software (Hamamatsu Photonics). Neurons were identified using both morphological and physiological criteria, specifically the expression of sodium and potassium currents and their capability to fire action potentials (APs) when properly stimulated by a current injection through the patch-electrode. Recordings were performed in the whole-cell configuration with a Multiclamp 700A amplifier and pClamp9 software (Molecular Devices). Series resistance was compensated up to approximately 80% and was generally below 10 MΩ. Patch micropipettes (3-4 MΩ) were filled with a solution (pH 7.3) containing (in mM): 130 potassium aspartate, 10 NaCl, 2 $MgCl_2$, 1.3 $CaCl_2$, 10 EGTA and 10 HEPES. The resting membrane potential (V_{rest}) was measured in each cell after establishing the whole-cell configuration. Action potentials were evoked by application of 1 sec-long depolarizing current pulses directly at V_{rest} or after hyperpolarizing the membrane at $\sim$ -75 mV. The depolarization peaks were considered action potentials when they were higher than 0 mV. Sodium and potassium currents were recorded in the voltage-clamp mode by depolarizing

the membrane from a holding potential of -90 mV to test potentials ranging from -80 to +20 mV.

PKH26 cell membrane labeling. hNSCs used in *in vivo* tests were previously tagged with PKH26 red fluorescent cell linker (Sigma) in accordance with the manufacturer's protocol. hNSCs were centrifuged at 300 g x 10 minutes and pellet was resuspended for 4 minutes in a PKH26 ethanolic dye solution (0.8% v/v). 1% of Bovine Serum Albumin (BSA, Sigma) in Hank's Balanced Salt Solution (HBSS, Euroclone) was added to stop the reaction. Cells were subsequently re-centrifuged and placed in a flask at concentration of 10^4 cells/cm^2 overnight. After 24 hours, cells were embedded in the 3D culture systems as previously described. Prior implantation *in vivo*, hNSC-HYDROSAP(1D) and hNSC-HYDROSAP(6W) were cultured *in vitro* for 1 day and 6 weeks respectively.

Dorsal hemisection model. 20 adult female Sprague-Dawley (SD) rats weighting 225g (Envigo Laboratories, Italy) were used. Surgeries were performed in sterile conditions. Due to health complications unrelated to the chosen treatment protocol (e.g. anaesthesia dose, etc) we had a few losses before the second surgeries, not considered in the results and immediately replaced with new animals: therefore, no animal that reached the end of the experimental timeframe was excluded in the results. For dorsal hemisection model, rats were deeply anesthetized with an intraperitoneal injection of ketamine (80 mg/kg) and xylazine (10 mg/kg). When unresponsive to toe pinch, the dorsal skin was shaved and an incision of the dorsal skin and a dorsal laminectomy were performed to expose the dura overlying the spinal cord at T9–T10 thoracic level. After identification of spinal cord midline, the vertebral column was stabilized by clamping the column at T8 and T11 vertebrae. A longitudinal cut, using a scalpel connected to Three-axis Joystick Oil Hydraulic Micromanipulator (Narishige) and surgical microscope (Zeiss), was made laterally from midline. Dorsal hemisection (at T9–T10 thoracic level) was created removing 3 x 1.5 x 1.5 mm hemicord. At 1 week after injury, all injured rats were randomized into four experimental groups (*n* = 5 per each group) and underwent a second operative procedure (see Table S14). Under the surgical microscope, the dorsal hemisection of spinal cord was cleaned from soft scar tissue (if present) and/or deposits,

then scaffolds were inserted into the lesion cavity. For SHAM-operated animals, saline only was used to fill the lesion cavity. A crossCK-made lamina (3 x 5 mm) was placed over the scaffold (and over the filled-cavity) and a mixture of 2 µl Fibrinogen (91mg/ml, Baxter) and 2 µl thrombin (500 U/ml, Baxter) was used to cover the dura opening. After dorsal hemisection, the overlying muscle and skin were closed with vicryl sutures and metal clips, respectively. To prevent host immune response to transplanted cells, CsA (50 mg/ml, Novartis) has been provided in the drinking water for 24 hours prior to surgery and continued for 8 weeks until sacrifice. For 1 week after surgery, all animals were daily injected subcutaneously with antibiotic (5 mg/kg, Enrofloxacin) to prevent infections and with Carprofen (4 mg/kg, Pfizer) to relive pain.

Rehabilitation and behavioral tests. Functional recovery was assessed by using the Basso, Beattie, Bresnahan (BBB) Locomotor Rating Scale (8). Scores were calculated according to the 0-21 point BBB scale for each hindlimb and averaged to give the animal an overall score. Locomotor activity was evaluated on day 3 post-initial injury and every 3/4 days until sacrifice. Each rat was observed for 4 minutes per each session. One week before first surgery all animals were familiarized to walk on the treadmill approximately at 10 meters/minutes (m/min). After implantation, two training sessions of a 6 m/min walk were performed during the first week. Later, treadmill speed was gradually increased (over consecutive sessions) up to 9 m/min (maximum speed) until the end of the experimental timeframe. The treadmill apparatus is combined with a SEDACOM software showing walked distance of each animal during each session. Walked distance was used as an indicator of animal performance, thus rehab sessions were also named treadmill test. All rats were tested individually for 10 min.

CSPGs quantification, immunohistochemical procedures and image analyses. At the end of *in vivo* experiments, eight weeks after second surgery, all rats were deeply anesthetized with an overdose of ketamine (120 mg/kg) and xylazine (14 mg/kg). Animals were sacrificed by cardiac perfusion under terminal anesthesia using 4% PFA. T8 - T12 spinal cord segments were explanted, post fixed in 4% PFA overnight and

cryopreserved in 30 % sucrose. 24 μm-thick longitudinal sections were cut serially via a cryostat, two per glass.

Following previously our published protocol (9) to quantify unsatured CSPGs disaccharides, longitudinal sections (including entire injury epicentre) were carefully detached from the glass slides and sonicated in PBS for 30 minutes. Spinal cord specimens were centrifuged at 3000 rpm for 3 minutes. Then, samples were loaded on TECAN Infinite M200 Pro Spectrophotometer for UV absorbance measurement (232 nm) of the unsatured CSPGs disaccharides. Optical densities (O.D) of readings were acquired and processed.

For immunohistochemical analyses, the procedure was performed similarly to the *in vitro* immunostaining. The following primary antibodies were used: βIII-TUB (1:500), GAP43 (1:100), GFAP (1:500), GABA (1:200), SMI31 (1:1000), VGLUT1 (1:100), MBP (1:3000), Ki67 (1:200), rabbit anti-von-willebrand factor (VWF) (1:500, Dako), rabbit anti-IBA1 (1:1000, Wako) and mouse anti- CD68 (1:500, Serotec).

Fluorescence images were captured at 20x magnification with Apotome Zeiss fluorescence microscope. Counting of PKH26^{+} cells was performed on serial spinal cord longitudinal sections in the lesion epicenter. Quantification of total number of PKH26^{+} cells per group was carried out using NIH-ImageJ software (> 60 images per each animal) and averaged over rats belonging to the same experimental group. Also, PKH26^{+} cells were used for normalization of neural markers expression of transplanted cells.

Morphometric quantification of gliosis size and axonal sprouting/regeneration in implanted spinal cord was performed on longitudinal sections using NIH-ImageJ software as previously described (10). Briefly, spinal cord sections were divided in rostral, central and caudal (352 µm to the lesion edge, three images for area). Gliosis and nerve markers were quantified on 54 images for each marker. Pixel area was converted to reactivity area in mm^2 and measurements of all sections were subsequently averaged in each animal.

Statistical Analysis. Results are reported as means ± SEM in all graphs. Data were processed using GraphPad Prism 7 software in *in vitro* and *in vivo* experiments, while Origin 8 (Microcal Inc., Northampton, Mass.) was used for the analysis of electrophysiological data. *In vitro tests* were performed in triplicate. Tunel assay, Ki67 and Nestin were evaluated by one-way ANOVA followed by Tukey's multiple comparison test. Cell differentiation and maturation were performed *via* two-way ANOVA followed by Tukey post-test. Statistical analysis between hNSC-HYDROSAP and CULTREX 3D were performed using two-way ANOVA followed by Bonferroni's multiple comparison test.

For electrophysiological analysis, statistical evaluations of the differences between the different cultures were obtained using the two-sample t-test or the two sample Kolmogorov-Smirnov Test and the Chi-square test.

$n = 5$ per each *in vivo* experimental group. BBB scores, body weight and treadmill training were analyzed by two-way ANOVA between groups over time followed by two-tailed t-test. Correlation between the BBB scores and body weight and between BBB scores and treadmill training was assessed using the Pearson method. Percentage of PKH26$^+$ cells and survival were analyzed by Unpaired t-test. CSPGs quantification, gliosis and nerve reactivity were evaluated by one-way ANOVA followed by Tukey's multiple comparison test. Statistical significance was set at $P < 0.05$.
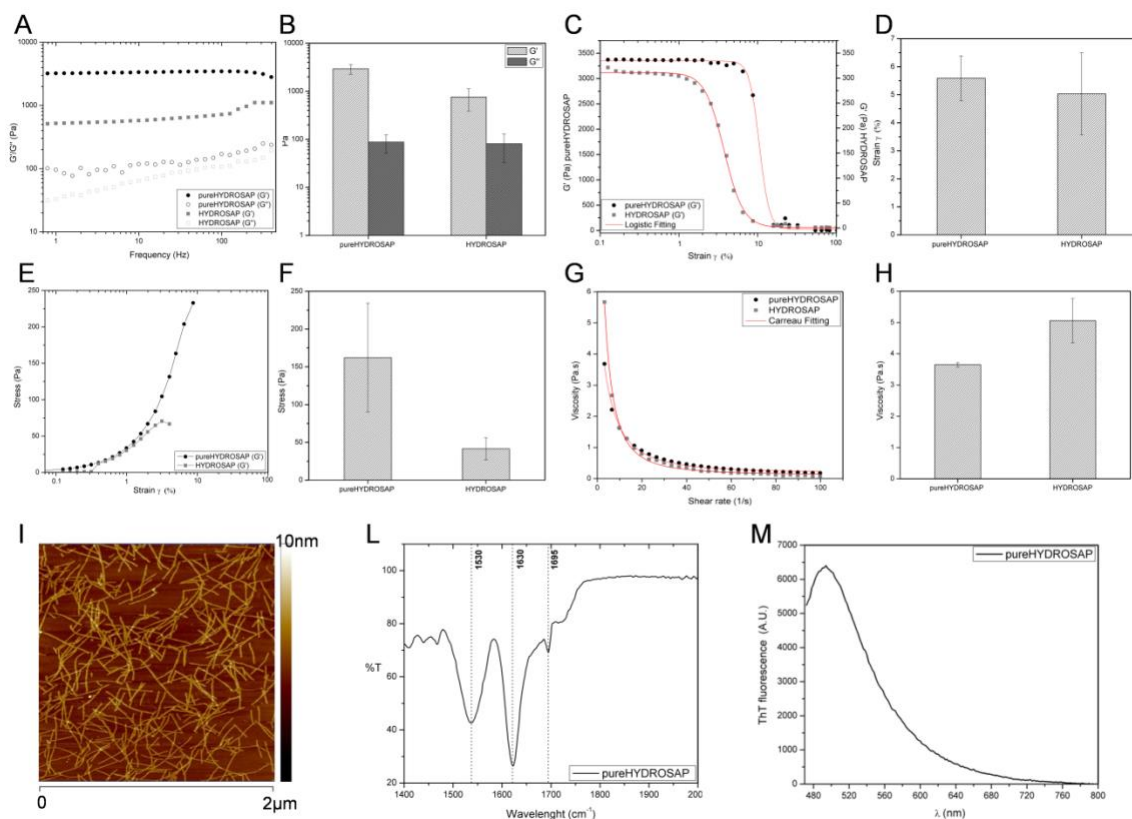
SUPPLEMENTARY FIGURES

Fig. S1. pureHYDROSAP and HYDROSAP characterization. **A to H** Rheological characterization of pureHYDROSAP and HYDROSAP. **A** Assembled peptide solutions were monitored by frequency sweep tests (0.1–100 Hz). Both peptides displayed typical hydrogel-like profiles featuring a predominant elastic solid-like (G'>G") behavior (G', solid dots), as compared with the viscous component (G", empty dots), with G' values of HYDROSAP lower than in pureHYDROSAP: this was not surprising as the decreased overall SAP concentration in HYDROSAP lowered the density of transient non-covalent interactions among assembled nanofibers. **B** Average G' and G" values of pureHYDROSAP and HYDROSAP in the 0.1-100Hz range. (**C and D**) Strain-failure test: both peptides were prone to deformation showing a typical strain-to-rupture of soft self-assembled hydrogel. **E and F** Stress-failure tests of assembled peptides. HYDROSAP showed a substantial failure stress decrease compared to pureHYDROSAP, likely due to perturbances on self-assembling given by sucrose, NaOH and cell culture medium. **G** Viscosity profiles of assembled pureHYDROSAP and HYDROSAP peptides

11

were measured as a function of continuous shear-rate ramps. (**H**) Both peptides showed typical trends of non-Newtonian fluids, but HYDROSAP exhibited higher viscosity values than pureHYDROSAP. Obtained experimental viscosities were fitted with the Carreau equation (red lines). (**I**) AFM morphological analysis. pureHYDROSAP peptide self-assembled into short nanofibers, displaying an average value in width and height of 13.84 ± 1.08 nm and 1.9 ± 0.29 nm. (**L**) Structural characterization of assembled scaffolds. ATR-FTIR spectrum in the Amide I and Amide II absorption regions of pureHYDROSAP peptide displayed a broad band at 1530 cm^{-1} (Amide II region), which is indicative of β-sheet aggregation, whereas peaks at 1630 cm^{-1} and 1695 cm^{-1} (Amide I region) suggest the presence of antiparallel β-sheet structures. **M** ThT spectroscopy assay. pureHYDROSAP showed an affinity for ThT ascribable to the presence of cross-β fibril structures.
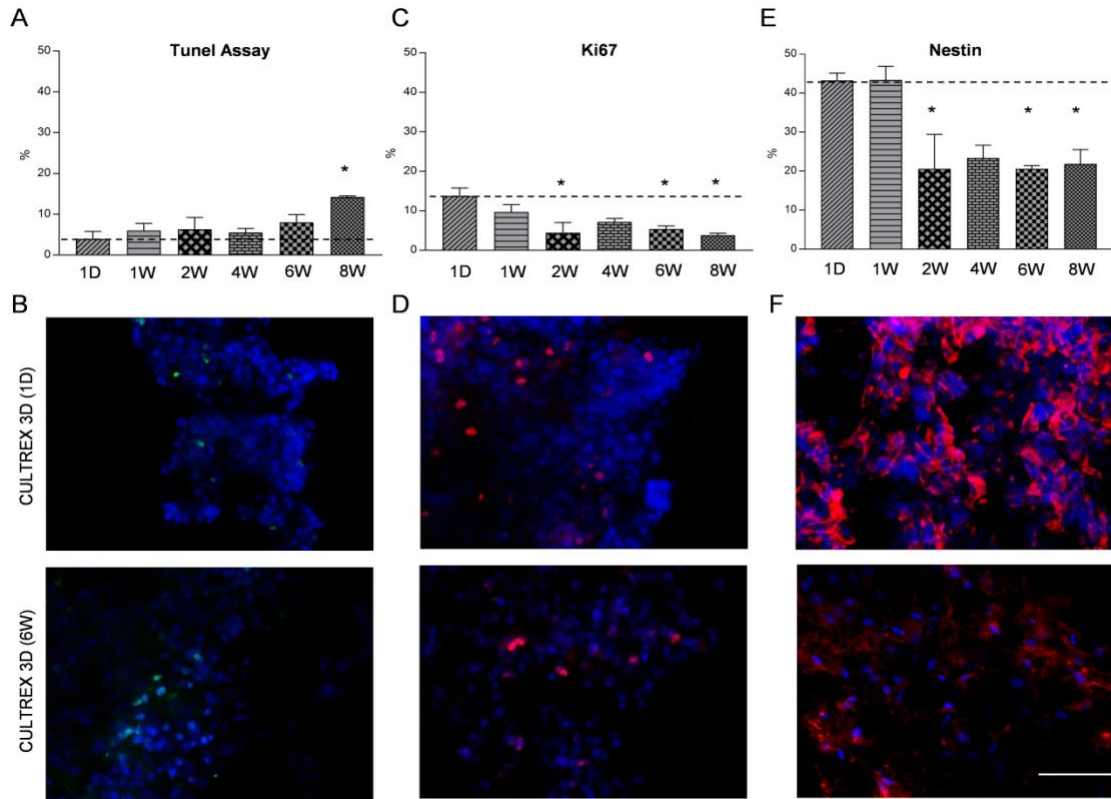
Fig. S2. TUNEL assay and immunostaining for respectively KI67 and Nestin of hNSCs cultured in CULTREX 3D. **A** Percentage of positive cells for Tunel Assay and **B** relative fluorescent images (in green) for CULTREX 3D (1D) and CULTREX 3D (6W). Results showed a small percentage of apoptotic cells in all experimental groups with a significant difference between CULTREX 3D (1D) and CULTREX 3D (8W) (*$P < 0.05$). **C** Graph related to percentage of Ki67-proliferative marker revealed decreased cell proliferation over time (1D vs 2W, 6W and 8W *$P < 0.05$). **D** Representative images after Ki67 staining (in red) for CULTREX 3D (1D) and CULTREX 3D (6W). **E** Nestin$^+$ cells in CULTREX 3D (1D) and CULTREX 3D (1W) were two-fold higher than all other groups; statistical analysis showed differences between CULTREX 3D (1D) and CULTREX 3D (1W) compared to CULTREX 3D (2W) and CULTREX 3D (6W) (*$P < 0.05$). **F** Differences between Nestin$^+$ cells (red) in CULTREX 3D (1D) vs CULTREX 3D (6W). Cell nuclei (DAPI) are labeled in blue. All graphs show mean ± SEM of triplicate samples per each timepoint. Dashed lines represent values of positive cells in CULTREX 3D at t = 0 days in vitro. Significant differences were detected by one-way ANOVA followed by Tukey post-test (*$P < 0.05$). Scale bar 50 µm.
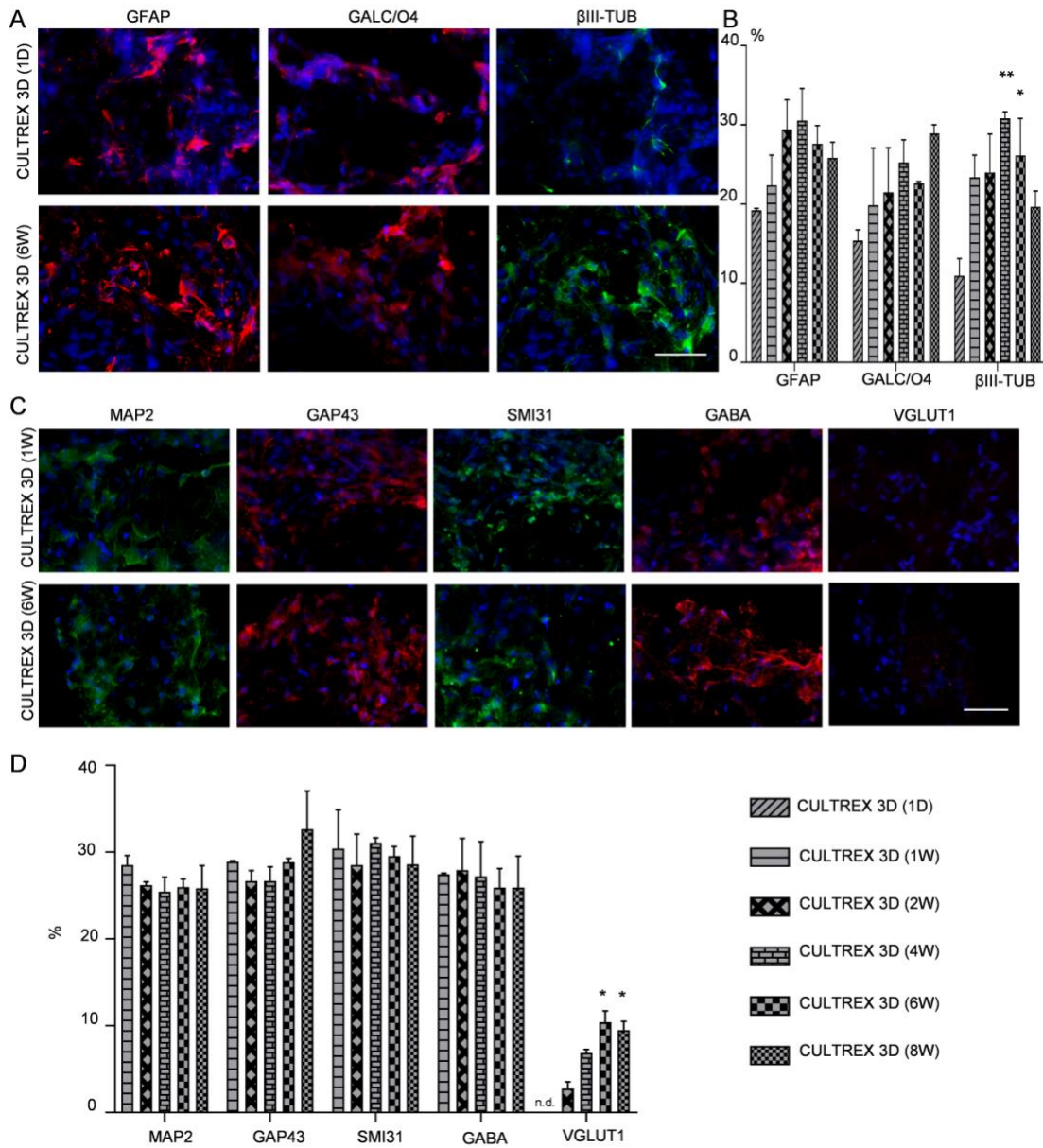
Fig. S3. Differentiation and maturation analysis of hNSCs cultured in CULTREX 3D. **A** and **B** Tri-lineage differentiation of hNSCs from 1 day to 8 weeks. Immunofluorescence images **A** for GFAP (red), GalC-O4 (red) and βIII-TUB (green) markers in CULTREX 3D (1D) and CULTREX 3D (6W). Percentages of positive cells for each marker were depicted in graph **B**. Significant differences in βIII-TUB expression were noticed for CULTREX 3D (4W) and CULTREX 3D (6W) (**$P < 0.01$ and *$P < 0.05$ respectively) compared to CULTREX 3D (1D). **C** and **D** Neuronal maturation analysis and expression of neurotransmitters of hNSCs from 1 week to 8 weeks. Representative

immunofluorescent pictures **C** for MAP2 (green), GAP43 (red), SMI31 (green), GABA (red) and VGLUT1 (red) positive cells in CULTREX 3D (1W) and CULTREX 3D (6W). Percentages of positive cells for each marker were depicted in **D**. Positive cells for VGLUT1 was not detected (n.d.) at 1 week. Significant differences were detected only for VGLUT1 marker (*$P < 0.05$ CULTREX 3D (1W) vs CULTREX 3D (6W) and CULTREX 3D (8W)). Statistical analysis: two-way ANOVA followed by Tukey multiple comparison test. All graphs show mean ± SEM (n=3). Cell nuclei (DAPI) are labeled in blue. Scale bar 50 µm.
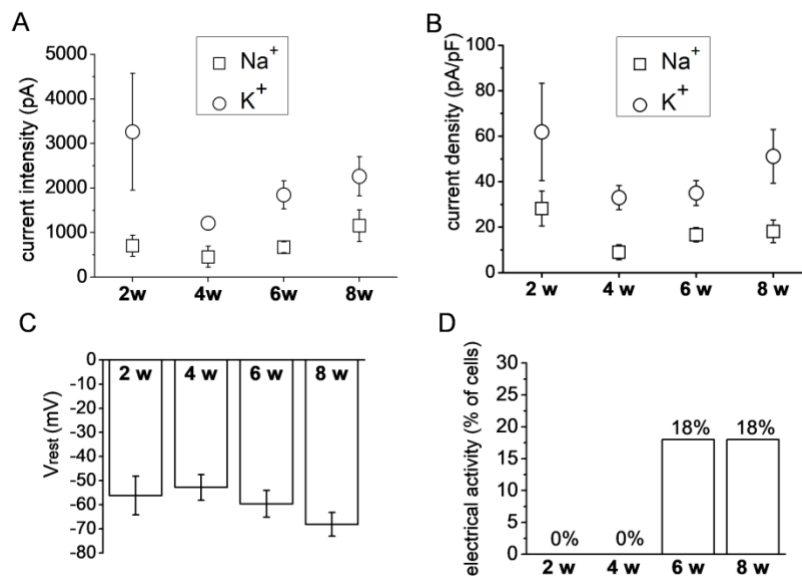
Fig. S4. Electrophysiological properties of hNSC in CULTREX 3D at different weeks of culture. **A** Mean sodium and potassium current amplitudes. Currents were evoked by membrane depolarization from a holding potential of -90 mV to test potentials ranging from -80 to +20 mV. **B** Mean sodium and potassium current densities. **C** Resting membrane potential (V_{rest}). **D** Percentage of cells endowed with electrical activity. Action potentials were present in CULTREX 3D starting from 6 weeks. See Table S1 for number of tested cells per week in culture.
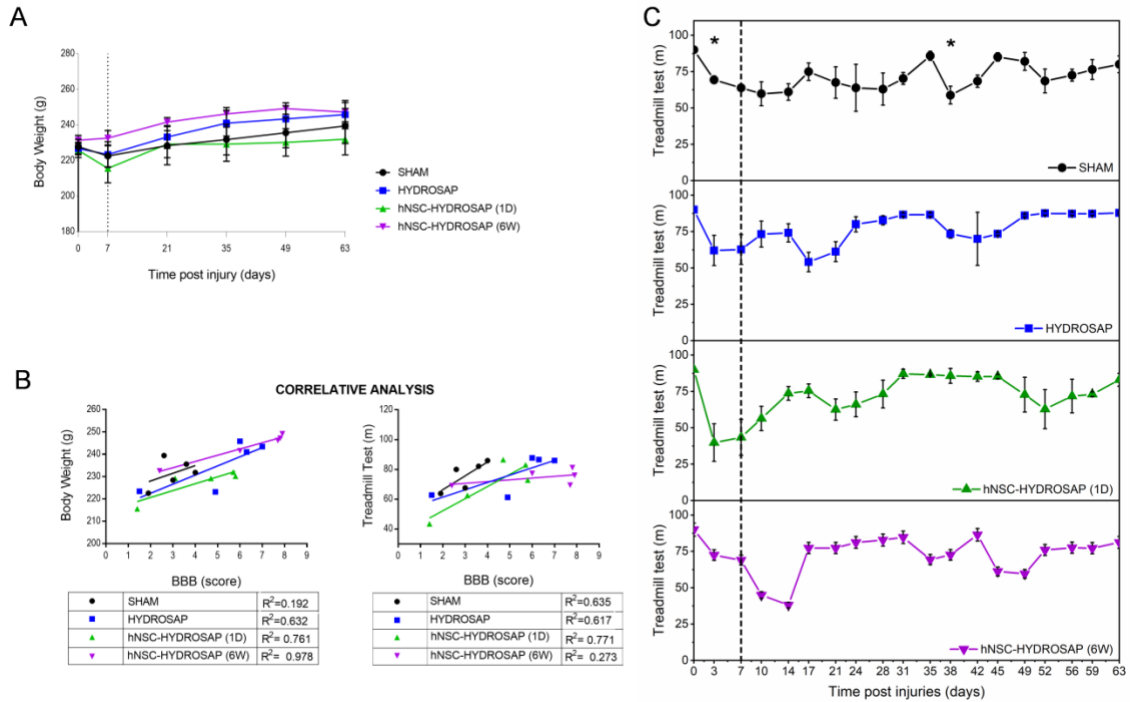
Fig. S5. Body weight gain tracking, body weight/BBB and treadmill/BBB correlative analyses and treadmill test. **A** All animals showed improved body weight gain in comparison to day 7 (implantation surgery, dotted line), with highest (but not statistically significant) values for hNSC-HYDROSAP(6W). **B** Positive correlations were found between body weight gain vs BBB score and treadmill test vs BBB score. R^2 values are listed next to their respective cohort. $n = 5$/group. **C** Treadmill test values converged toward a plateau representing the maximum walkable distance for the chosen rehab setup (i.e. the fixed treadmill speed). Dashed lines outline the day of implantation. hNSC-HYDROSAP(1D) group showed decreased walked distance at 3 days after injury, but after 38 days a significant value was detected compared to SHAM group. Data are presented as mean ± SEM, two-way ANOVA with Tukey post-hoc test evaluated statistical differences among the four groups over time ($n = 5$/group; *p < 0.05).
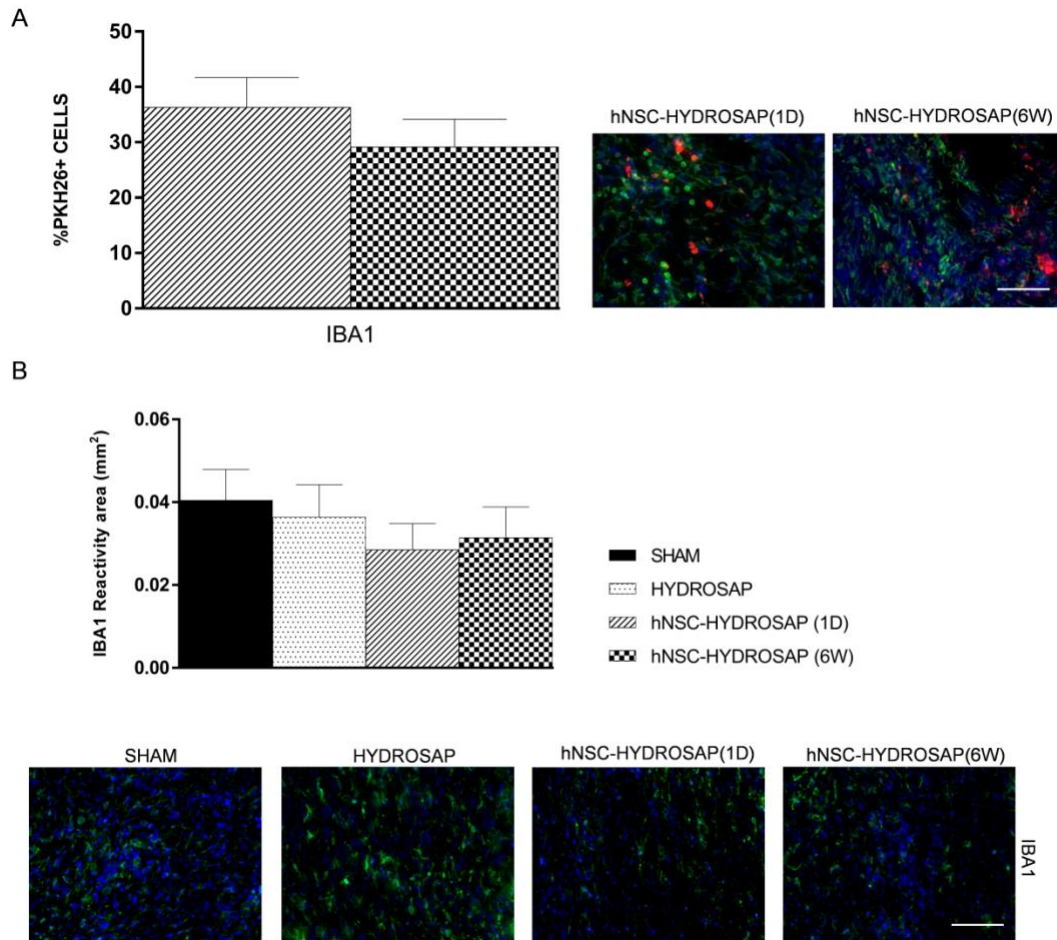
Fig. S6. Quantification of microglia/macrophage IBA1-marker in SHAM, HYDROSAP, hNSC-HYDROSAP(1D) and hNSC-HYDROSAP(6W) groups. **A** Percentage and representative images of PKH26$^+$ cells (red) co-localizing for IBA1 (green) in hNSC-HYDROSAP(1D) and hNSC-HYDROSAP(6W) experimental groups. No significant differences were detected. **B** Reactivity area and related immunofluorescent images of longitudinal sections of injured spinal cords showed cell density and morphology of IBA1$^+$ cells (green) in SHAM, HYDROSAP, hNSC-HYDROSAP(1D) and hNSC-HYDROSAP(6W). Quantifications pointed out no significant differences among all groups (one-way ANOVA followed by Tukey comparison test) ($n = 5$/group). Nuclei are stained with Hoechst (in blue). Scale bar 100 µm.
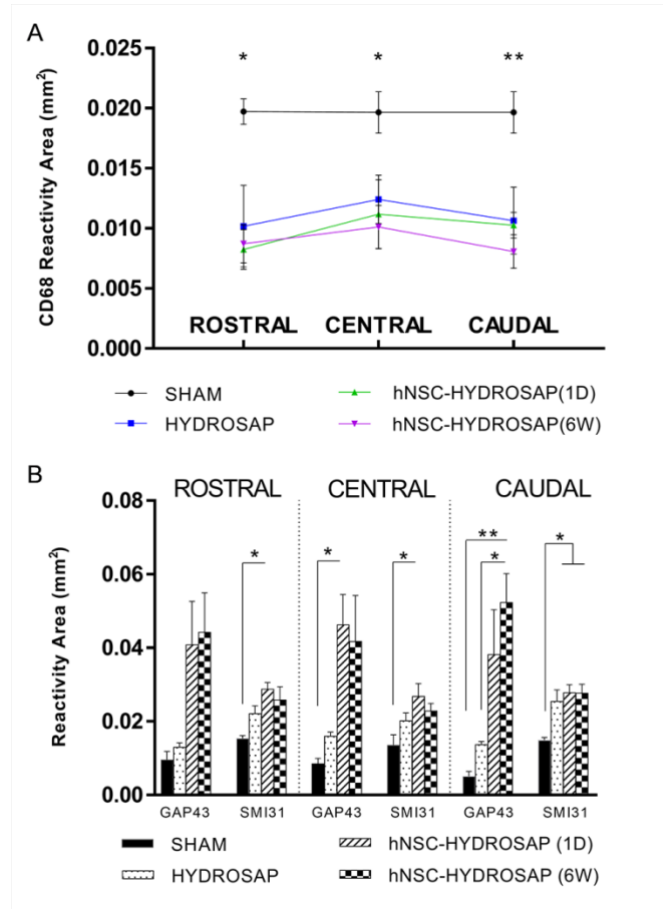
Fig. S7. Regionalized reactivity area for CD68, GAP43 and SMI31 markers in SHAM, HYDROSAP, hNSC-HYDROSAP(1D) and hNSC-HYDROSAP(6W). **A** Quantification of reactivity area of CD68 macrophage marker detected in regions rostral, central and caudal to the implantation site (longitudinal spinal cord sections). Significantly higher values for CD68 were observed in SHAM group compared to animals treated with hNSC-HYDROSAP (rostral: SHAM vs hNSC-HYDROSAP(1D) *P<0.05; central: SHAM vs hNSC-HYDROSAP(6W) *P<0.05; caudal: SHAM vs hNSC-HYDROSAP(6W) **P<0.01) (one-way ANOVA with Tukey post-hoc test, n = 5/group). **B** Quantification of regionalized reactivity areas positive for GAP43 and SMI31 markers. Statistical analysis revealed significant differences among SHAM and hNSC-HYDROSAP groups as well as for HYDROSAP vs hNSC-HYDROSAP(6W) (two-way ANOVA following by Tukey comparison test: *P < 0.05, **P < 0.01; n = 5/group).

18

SUPPLEMENTARY TABLES

Table S1. Statistical analysis of TUNEL ASSAY: CULTREX 3D vs hNSC-HYDROSAP

| Weeks | CULTREX 3D | | hNSC-HYDROSAP | | | |
	Mean	SEM	Mean	SEM	Significance	P Value
1D	3,994085	1,80496145	10,8361959	0,939625202	ns	0,63
1W	6,02137681	1,751427	24,55642276	4,745730204	***	<0,001
2W	6,36382179	2,88173321	24,56051851	2,863234605	***	<0,001
4W	5,517336783	1,004861	27,53053651	3,735711673	***	<0,001
6W	8,010752707	1,93513	24,39451431	4,399276318	**	0,003
8W	14,2217	0,304147	28,46938242	3,795943202	*	0,01

Two-way ANOVA followed by Bonferroni's multiple comparison test. ns stands for not statistically significant.

Table S2. Statistical analysis of KI67 immunostaining: CULTREX 3D vs hNSC-HYDROSAP

| Weeks | CULTREX 3D | | hNSC-HYDROSAP | | | |
	Mean	SEM	Mean	SEM	Significance	P Value
1D	13,73198	2,04351715	15,16825388	0,490959384	ns	>0,99
1W	9,68761862	1,871311	15,34068097	1,884464083	ns	0,10
2W	4,43719109	2,59984745	13,92895016	1,9137033	**	0,001
4W	7,207503467	0,846921	3,379175862	1,458276657	ns	0,55
6W	5,359944781	0,833556	2,147186959	0,276874355	ns	0,92
8W	3,82731	0,493882	4,283460455	1,67058606	ns	>0,99

Two-way ANOVA followed by Bonferroni's multiple comparison test. ns stands for not statistically significant.

Table S3. Statistical analysis of Nestin immunostaining: CULTREX 3D vs hNSC-HYDROSAP

| Weeks | CULTREX 3D | | hNSC-HYDROSAP | | | |
	Mean	SEM	Mean	SEM	Significance	P Value
1D	43,27931	1,85364456	36,6614709	1,934164228	ns	>0,99
1W	43,4131999	3,474942	37,33359052	1,640995508	ns	>0,99
2W	20,601605	8,84218247	18,61739348	0,313127331	ns	>0,99
4W	23,40058488	3,265202	20,04422617	2,767024624	ns	>0,99
6W	20,59224771	0,808468	15,34415218	2,35997358	ns	>0,99
8W	21,84889	3,665968	18,85620249	1,868910285	ns	>0,99

Two-way ANOVA followed by Bonferroni's multiple comparison test. ns stands for not statistically significant.

Table S4. Statistical analysis of GFAP immunostaining: CULTREX 3D vs hNSC-HYDROSAP

| Weeks | CULTREX 3D | | hNSC-HYDROSAP | | | |
	Mean	SEM	Mean	SEM	Significance	P Value
1D	19,21238	0,2446721	11,3051643	1,40805784	ns	0,31
1W	22,3909946	3,778196	28,81507056	3,202166828	ns	0,65
2W	29,4102649	3,77857187	32,99407839	1,157184821	ns	>0,99
4W	30,54361524	4,071407	29,35237969	2,414392835	ns	>0,99
6W	27,61821151	2,314377	32,92678697	2,369802701	ns	>0,99
8W	25,84749	1,967953	32,40650284	3,07281906	ns	0,61

Two-way ANOVA followed by Bonferroni's multiple comparison test. ns stands for not statistically significant.

Table S5. Statistical analysis of GALC/O4 immunostaining: CULTREX 3D vs hNSC-HYDROSAP

| Weeks | CULTREX 3D | | hNSC-HYDROSAP | | | |
	Mean	SEM	Mean	SEM	Significance	P Value
1D	15,37121	1,373664	0	0	*	0,01
1W	19,8355126	7,240989	18,04394923	2,634119916	ns	>0,99
2W	21,4760801	5,65253024	15,01149299	2,82313846	ns	0,94
4W	25,25510768	2,874772	12,7246183	1,181719331	ns	0,06
6W	22,65600598	0,178086	14,97567272	2,211042785	ns	0,57
8W	28,92847	1,083433	11,4044039	0,610395694	**	0,003

Two-way ANOVA followed by Bonferroni's multiple comparison test. ns stands for not statistically significant.

Table S6. Statistical analysis of βIII-TUB immunostaining: CULTREX 3D vs hNSC-HYDROSAP

| Weeks | CULTREX 3D | | hNSC-HYDROSAP | | | |
	Mean	SEM	Mean	SEM	Significance	P Value
1D	10,94919	2,15788656	6,31500502	1,284109255	ns	>0,99
1W	23,3693378	2,818835	22,56537409	1,960613187	ns	>0,99
2W	23,9694602	4,86682691	21,89814633	2,874173927	ns	>0,99
4W	30,8102076	0,827743	25,70487416	0,705429344	ns	>0,99
6W	26,15540096	4,671949	18,79826049	0,811636418	ns	0,42
8W	19,63627903	2,025925536	17,65687498	3,555773374	ns	>0,99

Two-way ANOVA followed by Bonferroni's multiple comparison test. ns stands for not statistically significant.

Table S7. Statistical analysis of MAP2 immunostaining: CULTREX 3D vs hNSC-HYDROSAP

	CULTREX 3D		hNSC-HYDROSAP			
Weeks	Mean	SEM	Mean	SEM	Significance	P Value
1W	28,5266974	1,079505	14,76474404	1,017035607	***	<0,001
2W	26,2326695	0,36718058	19,57081382	1,347494861	ns	0,05
4W	25,46443613	1,649156	19,93696704	1,004964423	ns	0,15
6W	25,97072201	0,93316	26,43812746	3,397134957	ns	>0,99
8W	25,83437	2,612246	24,76806272	0,772315377	ns	>0,99

Two-way ANOVA followed by Bonferroni's multiple comparison test. ns stands for not statistically significant.

Table S8. Statistical analysis of GAP43 immunostaining: CULTREX 3D vs hNSC-HYDROSAP

	CULTREX 3D		hNSC-HYDROSAP			
Weeks	Mean	SEM	Mean	SEM	Significance	P Value
1W	28,9299478	0,079391	22,50232892	3,18576359	ns	0,24
2W	26,679876	1,19672933	26,64503	2,065300138	ns	>0,99
4W	26,69493522	1,60779	35,22989014	1,461846839	ns	0,06
6W	28,86438788	0,403822	33,47903094	0,780582481	ns	0,73
8W	32,65139	4,407171	25,34800217	2,414197515	ns	0,13

Two-way ANOVA followed by Bonferroni's multiple comparison test. ns stands for not statistically significant.

Table S9. Statistical analysis of SMI31 immunostaining: CULTREX 3D vs hNSC-HYDROSAP

	CULTREX 3D		hNSC-HYDROSAP			
Weeks	Mean	SEM	Mean	SEM	Significance	P Value
1W	30,4088513	4,477943	18,47605949	2,06139488	*	0,01
2W	28,5281412	3,5630828	25,13240692	1,686013364	ns	>0,99
4W	31,0673454	0,566936	22,7485798	1,897418366	ns	0,14
6W	29,5521653	1,087922	23,73607551	1,480539598	ns	0,57
8W	28,62715	3,229063	24,45763092	2,129992875	ns	>0,99

Two-way ANOVA followed by Bonferroni's multiple comparison test. ns stands for not statistically significant.

Table S10. Statistical analysis of GABA immunostaining: CULTREX 3D vs hNSC-HYDROSAP

	CULTREX 3D		hNSC-HYDROSAP			
Weeks	Mean	SEM	Mean	SEM	Significance	P Value
1W	27,4370874	0,159233	25,79820593	1,382775297	ns	>0,99
2W	27,9437929	3,63036284	25,39507271	0,325616952	ns	>0,99
4W	27,23307104	3,980277	23,68002733	1,898797023	ns	>0,99
6W	25,90772158	2,193733	24,29720875	0,792645049	ns	>0,99
8W	25,90235	3,662356	24,62474199	2,068204748	ns	>0,99

Two-way ANOVA followed by Bonferroni's multiple comparison test. ns stands for not statistically significant.

Table S11. Statistical analysis of VGLUT1 immunostaining: CULTREX 3D vs hNSC-HYDROSAP

	CULTREX 3D		hNSC-HYDROSAP			
Weeks	Mean	SEM	Mean	SEM	Significance	P Value
1W	0	0	11,38335354	2,527505939	**	0,006
2W	2,777468	0,778686	13,83820215	0,722929595	**	0,008
4W	6,869755	0,418356	16,14587768	4,773632398	*	0,03
6W	10,40457	1,310218	18,74658608	2,211846231	ns	0,06
8W	9,511011	1,002153	22,4172606	2,866051286	**	0,002

Two-way ANOVA followed by Bonferroni's multiple comparison test. ns stands for not statistically significant.

Table S12. Electrophysiological properties of hNSC-differentiated cells cultured in CULTREX 3D, recorded via the patch-clamp technique.

Weeks in culture	N° of cells	Capacity (pF)	V_{rest} (mV)	I_{Na} (pA)	I_{Na} density (pA/pF)	cells with I_{Na}	I_K (pA)	I_K density (pA/pF)	cells with I_K	cells with AP
2	4	28 ± 11	-56 ± 8	703 ± 236	28 ± 8	100%	3262 ± 1310	62 ± 21	100%	0%
4	5	41 ± 7	-53 ± 5	455 ± 235	9 ± 3	100%	1213 ± 150	33 ± 5	100%	0%
6	13	47 ± 5	-60 ± 5	671 ± 121	17 ± 3	92%	1846 ± 314	35 ± 5	100%	18%
8	11	54 ± 9	-68 ± 5	1154 ± 357	18 ± 5	90%	2263 ± 440	51 ± 12	100%	18%

Table S13. Statistical analysis of BBB score data by two-way ANOVA with repeated measures.

DAYS	SHAM vs HYDROSAP	SHAM vs hNSC-HYDROSAP (1D)	SHAM vs hNSC-HYDROSAP (6W)	HYDROSAP vs hNSC-HYDROSAP (1D)	HYDROSAP vs hNSC-HYDROSAP (6W)	hNSC-HYDROSAP (1D) vs hNSC-HYDROSAP (6W)
0	ns (>0.99)	ns (>0.99)	ns (>0.99)	ns (>0.99)	ns (>0.99)	ns (>0.99)
3	ns (>0.99)	ns (>0.99)	ns (=0.87)	ns (>0.99)	ns (=0.83)	ns (=0.87)
7	ns (=0.98)	ns (0=.96)	ns (=0.96)	ns (>0.99)	ns (=0.83)	ns (=0.78)
10	ns (=0.91)	ns (=0.96)	ns (=0.83)	ns (>0.99)	ns (=0.42)	ns (=0.54)
14	ns (>0.99)	ns (>0.99)	ns (=0.48)	ns (=0.94)	ns (=0.66)	ns (=0.32)
17	ns (=0.91)	ns (=0.72)	ns (=0.16)	ns (=0.32)	ns (=0.48)	YES (=0.01)
21	ns (=0.27)	ns (>0.99)	YES (=0.02)	ns (=0.32)	ns (=0.72)	YES (=0.03)
24	ns (=0.32)	ns (=0.66)	ns (=0.08)	ns (=0.94)	ns (=0.91)	ns (=0.60)
28	ns (=0.37)	ns (=0.72)	ns (=0.06)	ns (=0.94)	ns (=0.83)	ns (=0.48)
31	ns (=0.10)	ns (=0.66)	YES (=0.007)	ns (=0.66)	ns (=0.78)	ns (=0.16)
35	ns (=0.13)	ns (=0.91)	YES (=0.003)	ns (=0.42)	ns (=0.54)	YES (=0.02)
38	YES (=0.02)	ns (=0.42)	YES (<0.001)	ns (=0.54)	ns (=0.72)	ns (=0.08)
42	YES (=0.02)	ns (=0.42)	YES (<0.001)	ns (=0.54)	ns (=0.66)	ns (=0.06)
45	YES (=0.01)	ns (=0.19)	YES (<0.001)	ns (=0.72)	ns (=0.54)	ns (=0.08)
49	YES (=0.007)	ns (=0.16)	YES (<0.001)	ns (=0.66)	ns (=0.83)	ns (=0.19)
52	YES (<0.001)	YES (=0.04)	YES (<0.001)	ns (=0.42)	ns (=0.87)	ns (=0.10)
56	YES (<0.001)	YES (=0.02)	YES (<0.001)	ns (=0.78)	ns (=0.72)	ns (=0.19)
59	YES (=0.010)	YES (=0.03)	YES (<0.001)	ns (=0.98)	ns (=0.42)	ns (=0.23)
63	YES (=0.007)	YES (=0.02)	YES (<0.001)	ns (>0.99)	ns (=0.32)	ns (=0.19)

ns stands for not statistically significant

Table S14. Schematic description of *in vivo* experimental design (n=5 per each group).

Experimental groups	INJURY	pureHYDROSAP	hNSCs
SHAM	+	-	-
HYDROSAP	+	+	-
hNSC-HYDROSAP(1D)	+	+	+
hNSC-HYDROSAP(6W)	+	+	+

REFERENCES

1. Gritti A, Cova L, Parati EA, Galli R, Vescovi AL (1995) Basic fibroblast growth factor supports the proliferation of epidermal growth factor-generated neuronal precursor cells of the adult mouse CNS. *Neuroscience letters* 185(3):151-154.

2. Gritti A*, et al.* (1999) Epidermal and fibroblast growth factors behave as mitogenic regulators for a single multipotent stem cell-like population from the subventricular region of the adult mouse forebrain. *The Journal of neuroscience : the official journal of the Society for Neuroscience* 19(9):3287-3297.

3. Galli R, Pagano SF, Gritti A, Vescovi AL (2000) Regulation of neuronal differentiation in human CNS stem cell progeny by leukemia inhibitory factor. *Developmental neuroscience* 22(1-2):86-95.

4. Gelain F*, et al.* (2012) New bioactive motifs and their use in functionalized self-assembling peptides for NSC differentiation and neural tissue engineering. *Nanoscale* 4(9):2946-2957.

5. Caprini A*, et al.* (2013) A novel bioactive peptide: assessing its activity over murine neural stem cells and its potential for neural tissue engineering. *New biotechnology* 30(5):552-562.

6. Pugliese R, Fontana F, Marchini A, Gelain F (2018) Branched peptides integrate into self-assembled nanostructures and enhance biomechanics of peptidic hydrogels. *Acta biomaterialia* 66:258-271.

7. Pugliese R, Marchini A, Saracino G, Zuckermann R, Gelain F (2018) Cross-linked self-assembling peptide scaffolds. *Nano Research* 11(1):586-602.

8. Basso DM, Beattie MS, Bresnahan JC (1995) A sensitive and reliable locomotor rating scale for open field testing in rats. *Journal of neurotrauma* 12(1):1-21.

9. Raspa A, Bolla E, Cuscona C, Gelain F (2018) Feasible stabilization of chondroitinase abc enables reduced astrogliosis in a chronic model of spinal cord injury. *CNS neuroscience & therapeutics*.

10. Raspa A*, et al.* (2016) A biocompatibility study of new nanofibrous scaffolds for nervous system regeneration. *Nanoscale* 8(1):253-265.